Acta Montanistica Slovaca
ISSN 1335-1788
actamont.tuke.sk

Development of a hardbanding material for drill pipes based on high-manganese steel reinforced with complex carbides

Pavlo PRYSYAZHNYUK[1], Michał MOLENDA[2], Taras ROMANYSHYN[3], Liubomyr ROPYAK[4], Liubomyr ROMANYSHYN[3] and Vasyl VYTVYTSKYI[5]*

Authors' affiliations and addresses:
[1] Department of Welding, Ivano-Frankivsk National Technical University of Oil and Gas, Ivano-Frankivsk 076019, Ukraine
e-mail: pavlo1752010@gmail.com

[2] Faculty of Organization and Management, Silesian University of Technology, 41-800 Zabrze, Poland
e-mail: michal.molenda@polsl.pl

[3] Department of Oil and Gas Field Machinery and Equipment, Ivano-Frankivsk National Technical University of Oil and Gas, Ivano-Frankivsk 076019, Ukraine
e-mail: tarasromanushun@gmail.com
e-mail: romanyshynl@gmail.com

[4] Department of Computerized Engineering, Ivano-Frankivsk National Technical University of Oil and Gas, Ivano-Frankivsk 076019, Ukraine
e-mail: l_ropjak@ukr.net

[5] Department of Engineering and Computer Graphics, Ivano-Frankivsk National Technical University of Oil and Gas, Ivano-Frankivsk 076019, Ukraine
e-mail: vytvytskyi.v.s@gmail.com

***Correspondence:**
Pavlo Prysyazhnyk, Department of Welding, Ivano-Frankivsk National Technical University of Oil and Gas, Karpatska 15,
tel.: +380 (342) 72-71-77
e-mail: pavlo1752010@gmail.com

Funding information:
Ministry of Science and Education of Ukraine Project D 8-21-P (RK 0121U109591)

Acknowledgement:
The authors thank Thermo-Calc Software AB company for supporting Ukrainian scientists during these difficult times by providing high-quality software and especially Therese Gustafsson for comprehensive advice. The authors are grateful to the Ministry of Science and Education of Ukraine for the grant to implement project D 8-21-P (RK 0121U109591).

How to cite this article:
Prysyazhnyuk, P., Molenda M., Romanyshyn, T., Ropyak, L., Romanyshyn, L., & Vytvytskyi, V. Development of a hardbanding material for drill pipes based on high-manganese steel reinforced with complex carbides. *Acta Montanistica Slovaca,* Volume 27 (3), 685-696.

DOI:
https://doi.org/10.46544/AMS.v27i3.09

Abstract
In the present study, the new "casing-friendly" hardbanding alloy based on high-manganese steel reinforced with complex carbide particles was developed by combining thermodynamic modelling within the CALPHAD approach and first-principles calculations. The alloy, deposited by flux cored arc welding on a steel substrate, has a composite structure consisting of manganese-austenite with the ability to work hardening, fine (up to 5 µm) inclusions of the multi-component carbide (Nb, Ti, Mo, V) and C the thin layers of (Mo,V)C at the austenite grain boundaries. The comparative wear tests carried out with commercially available hardfacing materials of the Fe-W-C and Fe-Cr-C systems showed that the proposed alloy has the best combination of properties preventing the wear of the drill casing, while its abrasion resistance, as well as wear resistance in sliding friction conditions by steel counter body, is close to hypereutectic high chromium alloys. The microhardness tests performed on deformed specimen areas after the friction tests show the presence of a significant hardness gradient in the range of 800-450 HV at a distance of about 300 µm when moving perpendicularly away from the zone of friction contact. During the microscopic observation of the layer deposited with the developed alloy and the interfaces between the deposit and the base steel, no cracks or pores delamination were detected, indicating a strong metallurgical bonding. The hardbanding process was performed for drill pipe joints with the worn Fe-based high chromium alloy hardbanding after exploitation, which allows the drill pipe to be re-used with the same durability.

Keywords
Thermodynamic modelling, hardbanding, drilling pipes, high-manganese steel, high-chromium coating, complex carbides.

Introduction

Equipment used during drilling, production and transportation of oil and gas is operated in difficult conditions: at high temperatures and exposed to dynamic alternating loads in aggressive corrosive environments containing solid abrasive particles of rock. The introduction of advanced technologies for drilling wells and hydrocarbon production requires modern equipment and tools with high performance (Bazaluk et al., 2022; Bazaluk, Slabyi, et al., 2021; Dychkovskyi et al., 2020; Khouri et al., 2016; Kovanič et al., 2021; Kovanič et al., 2021; Pukanská et al., 2017; Romanyshyn et al., 2020; Teodoriu & Bello, 2021). One of the main requirements for the technical condition of drilling, casing and pipe columns is the tightness and reliability of threaded connections during the life cycle (Kopei et al., 2019; Onysko et al., 2020) since leaks of petroleum products or natural gas cause a number of environmental problems (Mandryk et al., 2020). Threaded joints are typical thin-walled constructions that operate under extreme conditions and are one of the drilling string's weakest and most important components.

A number of design, technological and operational methods are used to increase the life of threaded joints of the drill pipe string. When designing, special attention is paid to the rational selection of materials and coatings (Pashechko et al., 2017; Shihab et al., 2020; Shyrokov et al., 2009), investigation of corrosion processes (Saakiyan et al., 1987), wear measurements (Bembenek et al., 2020) and to the study of stress distribution in laminated bodies with functional coatings (Ropyak et al., 2020). In the article (Shats'kyi, 2015), the problems of annealing crack-like defects are taken into account by applying non-contrasting hardfacing material.

Technological methods ensure the achievement of manufacturing accuracy (Kopei et al., 2021; Medvid et al., 2020; Pryhorovska & Ropyak, 2019; Peterka, J. et al., 2008) and the quality of the working surfaces of bolted joints (Kopei et al., 2020; Ropyak et al., 2021), including taking into account technological inheritance (Kusyi & Kuk, 2020) since errors in their manufacture lead to increased stresses assembled structures (Bazaluk, Velychkovych, et al., 2021, Vaclav, S. et al., 2007). With the help of various types of composite-type coatings, the life of the drill string is extended. The results of theoretical studies on the structure of metals (Levchuk et al., 2021; Melnick et al., 2020; Radchenko et al., 2020; Tatarenko & Radchenko, 2003) form the basis for the development of new materials and hardening technologies.

Operational methods include a scientifically based choice of operation of tubular columns with drill pipe joints, taking into account force interaction (Levchuk, 2017; Moisyshyn et al., 2012) and ensuring stable flushing of drilling tools in the borehole (Vytyaz et al., 2015). In order to create safe working conditions for drill string joints, damping and vibration protection devices are used (Shats'kyi et al., 2021), as well as rational methods for eliminating tool seizures in emergencies (Moisyshyn & Levchuk, 2016).

In many cases, the threaded connection is the weakest link in the drill string, and very often, emergencies or accidents result from the failure of these threaded connections due to corrosion and mechanical wear. Therefore, arc hardfacing is promising, among other things, to increase the service life of drill pipe joints.

Hardbanding is known as the process of applying wear-resistant alloys to drill pipe joints, primarily by arc welding, with the aim of increasing drill string service life. The drill pipe joints operating in contact with the casing can be represented as a friction couple working under severe sliding conditions complicated by the presence of an abrasive environment and impact loads. Such conditions become more complex in cases where heavy weight drill pipe (HWDP) is used (Murthy et al., 2011) or the well has significant deviations from the vertical direction. This makes the selection of the hardbanding material a non-trivial task, as high abrasion resistance must be combined with providing low wear rates of the casing mating body, i.e. deposited layer should be "casing-friendly" (Zhang et al., 2020). Recent experience with the use of tungsten carbide-based hardbanding materials shows that, despite extremely high abrasion resistance, the use of such deposited coatings leads to significant wear of the casing. This is mainly caused by microstructural features of the deposited layer, where coarse-grained particles of tungsten carbide act as micro-cutters in relation to the drill string casing. As an alternative, "casing-friendly" hardbanding materials based on the Fe-Cr-C alloying system (Caltaru et al., 2020) are commercially available as products from Anrco Company's of XT grades. Disadvantages of that type of coatings are typical for the Fe-based hypereutectic high-chromium alloys, including low impact resistance and coarse microstructure. Coatings of this type suffer from the same disadvantages as most Fe-based hypereutectic hardfacing alloys, including poor resistance to impact loads and a coarse carbide microstructure. A more advanced approach to developing hardbanding materials by using complex alloying with such strong carbide-forming elements as Ti, Nb and shown in (Haberer et al., 2014). The resulting deposited layers have a fine microstructure represented by uniformly distributed fine carbide particles within the low-carbon steel matrix. The abrasion wear resistance of Nb and Ti alloyed hardbanding exceeds the wear resistance of typical high chromium hardfacing by four times, although their hardness (53 HRC) is lower at 4-6 HRC. This suggests that hardness is not a key factor in ensuring wear resistance, but the formation of a composite matrix-reinforced surface layer fine structure under such conditions plays a crucial role. Such a structure can be achieved through the development of complex alloying systems that include high-alloyed steels and multi-component carbide phases (Segota et al., 2020). Twinning-induced plasticity (TWIP) type austenitic steels are promising materials for use as the steel matrix phase for hardbanding coatings due to their high impact

wear resistance and good weldability in a wide range of welding modes. The transition metal carbides such as TiC, NbC, Mo_2C, VC, etc., characterized by the formation of stable multi-component interstitial phases that crystallize in the form of dispersed inclusions with high microhardness (> 20 GPa), are promising as reinforcement.

The aim of the present investigation is the development of a new hardbanding material in the form of flux cored wire for arc cladding that offers a composite structure of the surface layers consisting of a high manganese austenitic TWIP steel matrix reinforced with hard multi-component carbides. In particular, this study aimed at a thermodynamic analysis of the promising alloy systems using the CALPHAD technique to find the relationship between the alloy composition and the amounts of desired phases.

Theoretical background

The robust technique that enables the development of multiphase materials with the desired phase composition and properties is the CALPHAD (CALculation of PHAse Diagrams) approach, which is based on minimizing the total Gibbs free energy of the system by comparing the thermodynamic properties of its competing phases calculated according to the Compound Energy Formalism (CEF), suggested by M. Hillert (Hillert, 2001). For example, according to CEF, the Gibbs energy of manganese austenite and carbides of Ti, Nb, and V with the NaCl structure and other similar solid solutions can be represented by a two-sublattice model, with one sublattice filled with metal atoms, while the other is filled with carbon and vacancies. In this case, the Gibbs energy for a formula unit of a phase is described by the following equation:

$$G_M^f = \sum_i y_i\left(y_C\ {}^{\circ}G_{i:C}^{\phi} + y_{va}\ {}^{\circ}G_{i:va}^{\phi}\right) + RT\sum_i y_i\, ln(y_i) + cRT(y_C\, ln(y_C) + y_{va}\, ln(y_{va})) + {}^{mg}G^{\phi} + {}^{E}G_M^{\phi}, \quad (1)$$

where y_i, y_c and y_{va} are the site fractions of the *i*-th metal component, carbon and vacancies, respectively; ${}^{\circ}G_{i:va}^{\phi}$ and ${}^{\circ}G_{i:C}^{\phi}$ are the Gibbs energies of the pure components and carbide phases with the given structure, respectively; c denotes the number of free lattice sites (tetrahedral and octahedral pores) with respect to one metal atom; ${}^{mg}G^{\phi}$ is the magnetic contribution to the Gibbs energy and ${}^{E}G_M^{\phi}$ is the excess energy of mixing. For a system containing three metal components (i, j and k), carbon and vacancies (va), excess energy can be expressed as:

$$\boldsymbol{{}^{E}G_M^{\phi} = \sum_i\sum_j y_i y_j\left(y_C L_{i,j:C}^{\phi} + y_{va} L_{i,j:va}^{\phi}\right) + y_C y_{va}\sum_i y_i L_{i:C,va}^{\phi} + \sum_i\sum_j\sum_k y_i y_j y_k\left(y_C L_{i,j,k:C}^{\phi} + y_{va} L_{i,j,k:va}^{\phi}\right),\ i \neq j \neq k\,,} \quad (2)$$

where:
L are the composition and temperature-dependent second and third-order interaction parameters (excess terms) that can be evaluated using the Redlich-Kister (RK) (Redlich & Kister, 1948) n-order polynomials:

$$L_{i:C,va}^{\phi} = \sum_{n=0}^{v} {}^{n}L_{i:C,va}^{\phi}(y_c - y_{va})^n\,, L_{i,j:C}^{\phi} = \sum_{n=0}^{v} {}^{n}L_{i,j:C}^{\phi}\left(y_i - y_j\right)^n,$$
$$L_{i,j:va}^{\phi} = \sum_{n=0}^{v} {}^{n}L_{i,j:va}^{\phi}\left(y_i - y_j\right)^n. \quad (3)$$

The thermodynamic parameters for the substitution in Eq. (1) and Eq. (3), except for Mo-containing phases, were mainly taken from the (Hallstedt et al., 2017); other parameters were selected using the TDB-DB search system (Walle et al., 2018, Cernecky et al., 2015). The unknown important excess terms ($L_{i,j:C}^{\phi}$) that determine the solubility of Mn in carbide phases were obtained using a special Quasi-Random (SQS) structure approach (van de Walle & Asta, 2019) implemented in ATAT software (Walle & Ceder, 2002) in sqs2tdb module (Walle et al., 2017). The required first-principles energy calculations were performed using the Quantum Espresso v.7.0 software (Giannozzi et al., 2009) with GBRV v.1.5 set of ultrasoft pseudopotentials (Garrity et al., 2014). All the thermodynamic calculations were performed using the Thermo-Calc 2022a software (Andersson et al., 2002).

Materials and Methods

Specimens for experimental testing were prepared by hardfacing using the Flux-Cored Arc Welding (FCAW) technique with cored wires filled with alloy components. Commercially available powders of NbC, VC, Mo_2C and TiC with irregular morphology and particle size ranging from 5 to 500 μm were used as starting carbide components, as shown in Fig. 1.

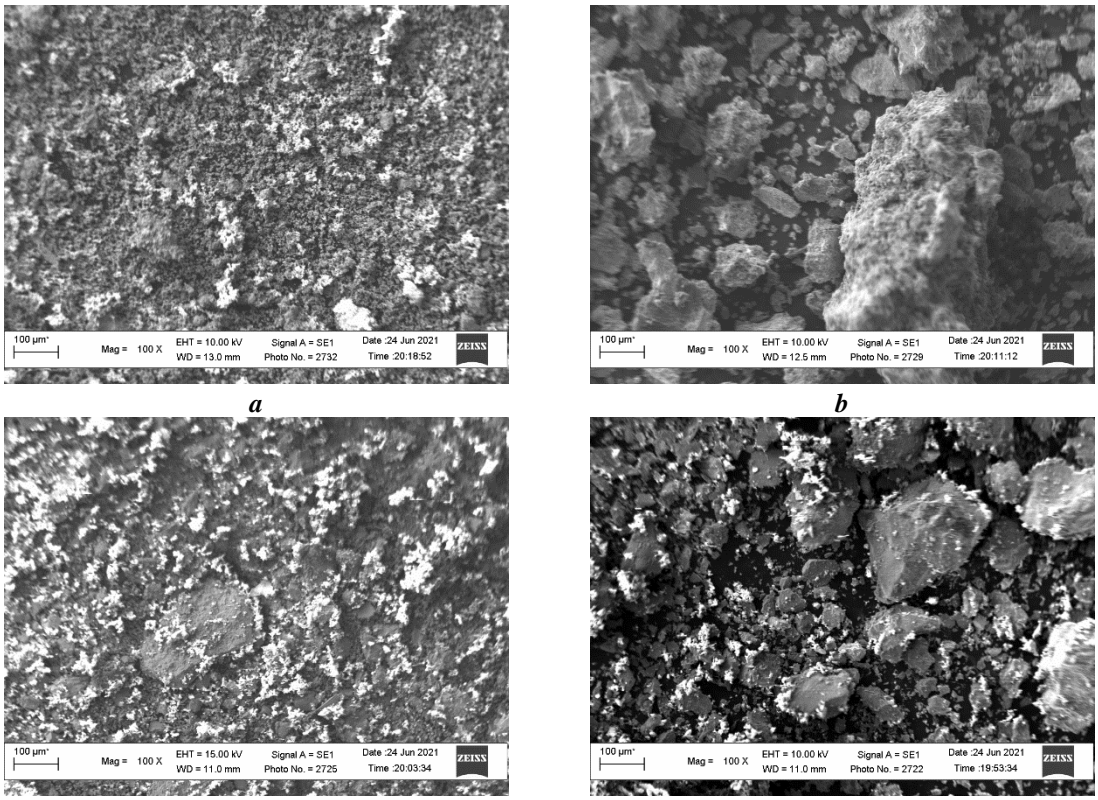

Fig. 1 The morphology of initial carbide powders

Cemented carbide powders were mixed with ferromanganese (grade MNS17) and arc protection components (fluorite and rutile) in a drum mixer to obtain a homogeneous powder mixture, which was drawn into a low carbon steel sheath to obtain a cored wire with geometry parameters shown in Fig. 2. The flux-cored wire prepared as described above was coiled on a spool, whereby it could be used for hardbanding process by automatic arc welding. Deposition of the wear-resistant layers by FCAW was carried out on a plain carbon steel substrate with reversed polarity and a welding current of 160-180 A.

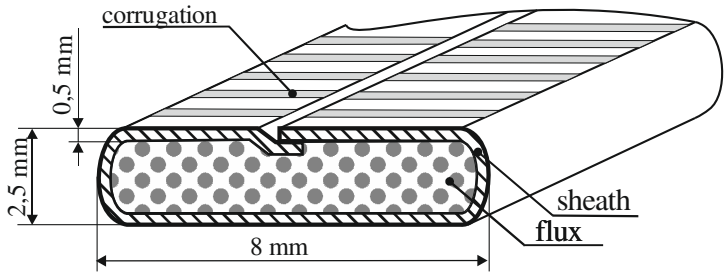

Fig. 2. The scheme of the cross-section of the cored wire

To investigate the structure, properties and wear resistance, test specimens with dimensions of 10×20×40 mm were cut from hardfaced plate. Microstructure observations of deposited layers were performed by scanning electron microscopy (SEM) together with energy dispersive X-ray spectroscopy (EDS) using a ZEISS EVO 40 XVP electron microscope. X-ray diffraction patterns for phase identification were performed using a DRON-3 diffractometer (Kuric, et al., 2022). The macro hardness of the deposited layers was measured by the Rockwell method (scale A), and the microhardness with a Vickers pyramid indenter at a load of 1 N on the cross sections of the deposited layers. The abrasion wear resistance of the hardfaced layers was determined by ASTM G65-04 standard test method for measuring abrasion using the dry sand/rubber wheel apparatus in the silica sand environment. To evaluate the ability of the hardbanding layer to ensure the durability of the case, the wear tests were performed according to the block (cylinder)-on-ring scheme using the modified SMTs-2 type tribometer. The loading of the friction couple was ensured by a system of two two-armed levers, as shown in Fig. 3. The rotation speed of the armoured disc was 300 rpm, while the load of the friction couple was set at 300 N, and the duration of each experiment was 30 min. In order to create friction conditions similar to the real drill pipe joint-casing pair, the water-based drilling fluid was used as the working environment. The wear rates of the test samples were

measured by weighing them before and after wear tests with an accuracy of 1 mg. To unify wear rates for materials with different densities, weight loss was converted to volume loss (Kuric, et al., 2020). T-590 grade high chromium hardfacing alloys and Lastek 210 grade tungsten carbide-based electrodes were selected to compare the properties of the developed material to commercially available hardbanding materials.

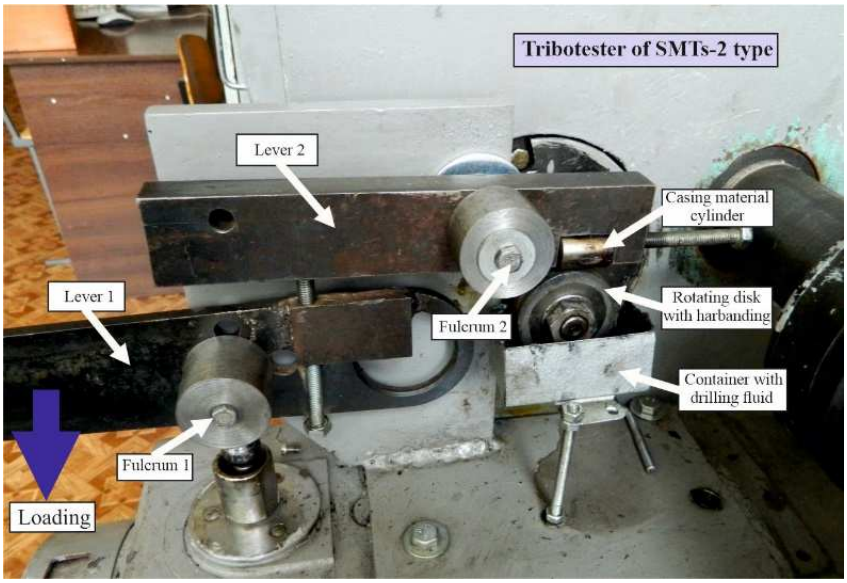

Fig. 3. The general view of the hardbanding materials testing machine using block (cylinder) on ring scheme

Results

The thermodynamic parameters ($L^{\phi}_{i,Mn:C}$) necessary for prediction of the phase composition of the hardbanding alloy assessed by *ab initio* calculations using the ATAT software are listed in Tab. 1.

Tab. 1. The calculated thermodynamic parameters for the carbides

Parameters (J/mole)	Parameters (J/mole)	Parameters (J/mole)	Parameters (J/mole)
${}^{0}L^{\phi}_{Ti,Mn:C} = +30048{,}4$	${}^{0}L^{\phi}_{V,Mn:C} = +9293{,}5$	${}^{0}L^{\phi}_{Nb,Mn:C} = +49286{,}6$	${}^{0}L^{\phi}_{Nb,Mn:C} = -8970{,}2$
${}^{1}L^{\phi}_{Ti,Mn:C} = +47056{,}9$	${}^{1}L^{\phi}_{V,Mn:C} = +22155{,}0$	${}^{1}L^{\phi}_{Nb,Mn:C} = +29600{,}7$	${}^{1}L^{\phi}_{Nb,Mn:C} = +2629{,}2$
${}^{2}L^{\phi}_{Ti,Mn:C} = -83870{,}8$	${}^{2}L^{\phi}_{V,Mn:C} = -71877{,}7$	${}^{2}L^{\phi}_{Nb,Mn:C} = -14537{,}4$	${}^{2}L^{\phi}_{Nb,Mn:C} = -11774{,}1$

As a starting point for the selection of the experimental hardbanding alloy composition, a pseudobinary section of the multi-component carbide-high manganese steel system was constructed (Fig. 4a). As can be seen from the figure, the stable phases in the most important areas are liquid high manganese austenite, MC-type complex carbides with face-centred lattices and (Mo,V)C (η-carbide). The optimal composition for the experimental hardbanding alloy was chosen for reasons of the existence of a broad two-phase region in which liquid and MC-type carbide exist in equilibrium, which coincides with the eutectic point at 68 vol. % high manganese steel (Wiecek, et al., 2019). The solidification process of the experimental alloy (Fig. 4b) starts with the crystallization of the complex (Nb,Ti,Mo,V)C-carbide, which starts at ~ 2600 K and the amount of which increases up to 20 vol % at 1580 K. At this temperature, a eutectic reaction takes place, followed by an intense increase in the proportion of austenite up to 70% vol. % and partial decomposition of the carbide phase, resulting in the formation of the new MC-type carbide phase enriched in V and Mo (Kopas, et al., 2017). Further cooling in a solid state does not lead to phase composition changes up to 1000 K, where MC-type carbide becomes unstable and transforms into η-type carbide (Burduk, et al., 2019). After all phase transitions are completed and considering the stability of the austenite caused by the presence of a high amount of Mn, the resulting predicted structure consists of three main phases, namely manganese-austenite (~ 68 vol. %), multi-component (Nb,Ti,Mo,V)C-carbide (~ 18 vol. %) and η-type (Mo,V)C carbide (~ 14 vol. %).

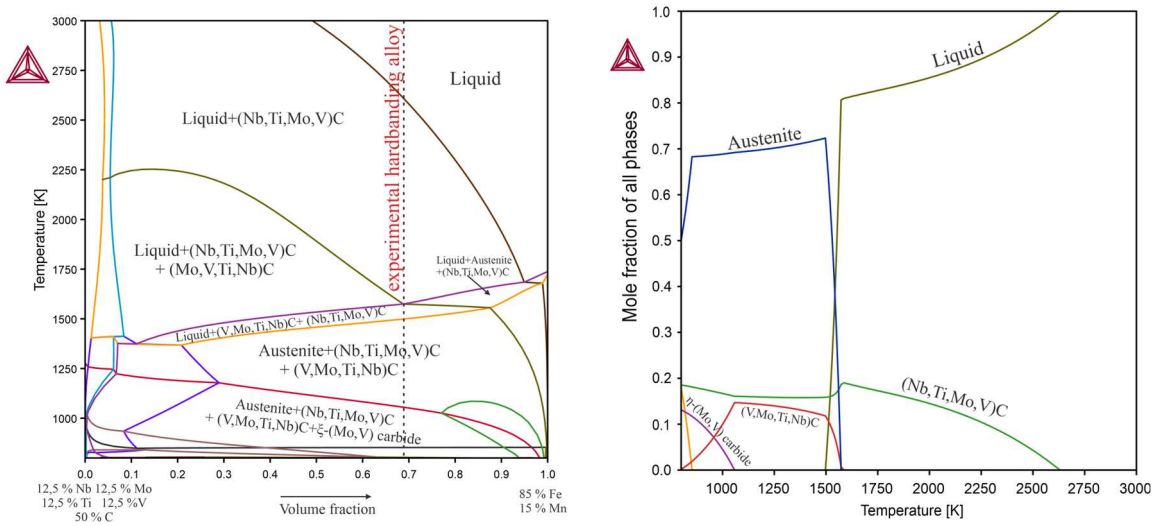

a *b*

Fig. 4. The calculated pseudobinary section of the hardbanding alloying system (a) and the temperature dependence of the phase composition for the selected hardbanding alloy

According to the results of thermodynamic modelling, the selected composition of the experimental alloy was recalculated to the required flux components of the cored wire considering its morphology features (Fig. 1, a d) and the construction of the cored wire (with a filling coefficient of 0,6) at a given manufacturing process. As a result, the initial powder components were drawn into the steel sheath in the following weight amounts. %: ferromanganese – 15,6; TiC – 10,8; NbC – 19; VC – 11,4; Mo_2C – 18,6 and the mixture of CaF_2 and TiO_2 the rest. The results of the microstructure investigations of the layer deposited by FCAW show the presence of all phases, predicted by the thermodynamic modelling (Kuric et al., 2021, Abramov et al., 2015). As can be seen from Fig. 5, the structure of the deposited layer consists mainly of a steel matrix represented by manganese austenite and uniformly distributed carbide grains with an average size of 5 µm. The total amount of the reinforcing carbide phases distributed within the steel matrix measured by image analysis is ~ 30 % by volume (Klarák et al., 2022). The cuboid-shaped inclusions, identified by EDS as multi-component (Nb,Ti,Mo,V)C carbides, are characterized by a core-rim structure that indicates the redistribution of the carbide-forming elements during solidification. The central areas of the grains are mainly enriched in Nb and Ti (Sapietova et al., 2011), while the peripheral areas contain significant amounts of Mo and V, although traces of all carbide elements are present throughout the grain area. The carbide phase identified as a η-carbide with the formula unit close to $V_{0,35}Mo_{0,15}C_{0,5}$ precipitates at the austenite grain boundaries in the form of thin (up to 1 µm) discontinuous layers (Saga et al., 2020). The formation of the η-carbides at the austenite grain boundaries is caused by its solidification in the solid state (Fig. 4b) as a result of (V,Mo,Ti,Nb)C decomposition. The results of microstructural studies of the interface zone between the deposited layer and the base material (steel) show the smooth transition across the heat-affected zone, which is characterized by the absence of pores, cracks, delamination, and other similar defects. This indicates a strong metallurgical bond between the hardbanding and the base metal, making it possible to propose the experimental hardbanding alloy for industrial FCAW.

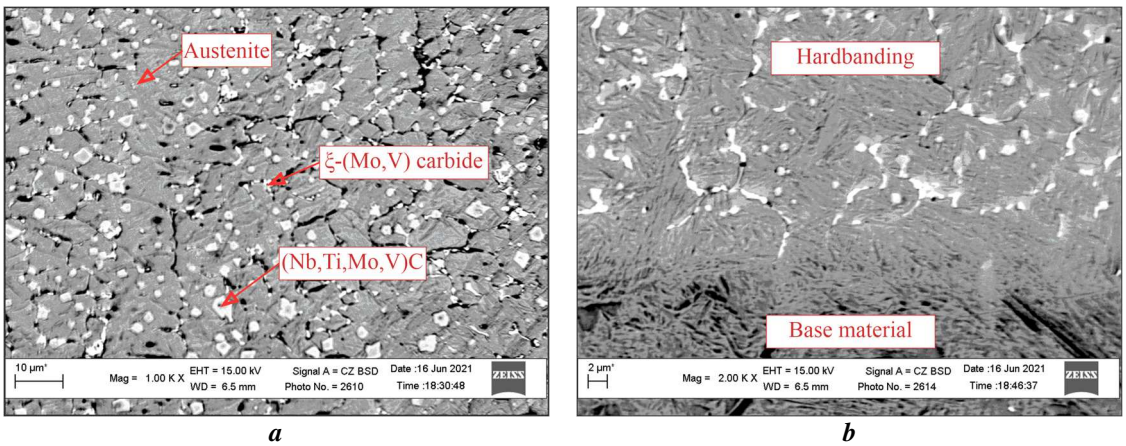

a *b*

Fig. 5. The microstructure of the hardbanding layer (a) and the interface between base steel material and deposited layer

The results of wear tests carried out on the machine shown in Fig. 3 show that WC-based hardbanding (Lastek 210) has the highest wear resistance in relation to all tested materials, despite the wear of the cylinder (imitating casing), and the coefficient of friction has the highest values. Discs with hardbanding based on high-chromium alloy (T-590) have higher volume loss compared to WC-based hardbandings, but counter body wear and friction coefficient are lower (Abd Ali et al., 2021). The use of an experimental hard-banding alloy makes it possible to achieve almost the same wear resistance values as an alloy with a high chromium content, but the properties that ensure the preservation of the efficiency of the case (coefficient of friction and volume loss of the cylinder) are the highest among all tested hardbanding materials (Handrik et al., 2017). Abrasion wear resistance tests performed according to the ASTM G65-04 standard show that tested materials by descending relative wear values can be ranged as follows: Lastek 210 – 4, T-590 – 1 and experimental alloy – 0,8.

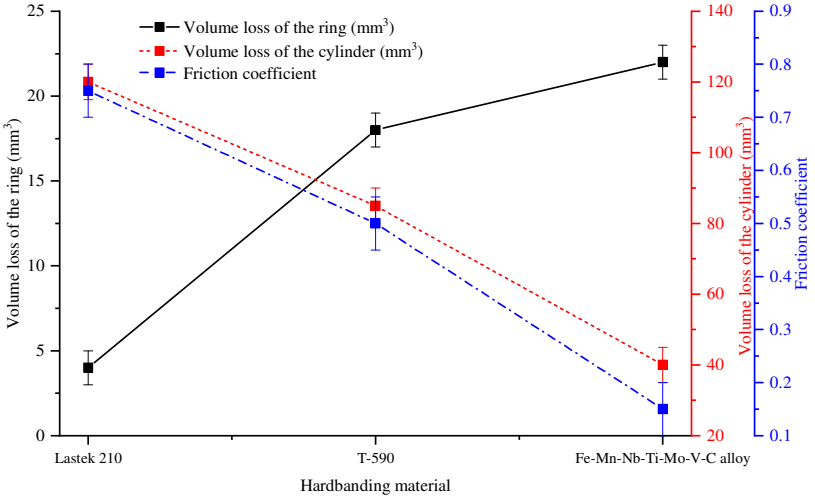

Fig. 6. The results of the wear tests of different hardbanding materials

The microstructural observations and microhardness measurements of the areas near the frictional contact zones of the disc with experimental hardbanding, carried out after the wear tests, show the presence of a microhardness gradient (Fig. 7) (Saga, Jakubovicova, 2014). The microhardness of the underlying layers related to the contact area is in the range of 700-800 HV at a distance of up to ~ 75 µm, while at a distance of 75-200 µm the microhardness values are in the range of 600-700 HV, and for distances above 200 µm, the microhardness is within 450-550 HV, which is close to the values of hardbanding after FCAW without deformation treatment (Saga, Blatnicky et al., 2020). Such presence of the hardness gradient indicates the occurrence of structural changes in a steel matrix, which occur in typical high manganese austenitic steels with an Mn content of more than 13 wt. %.

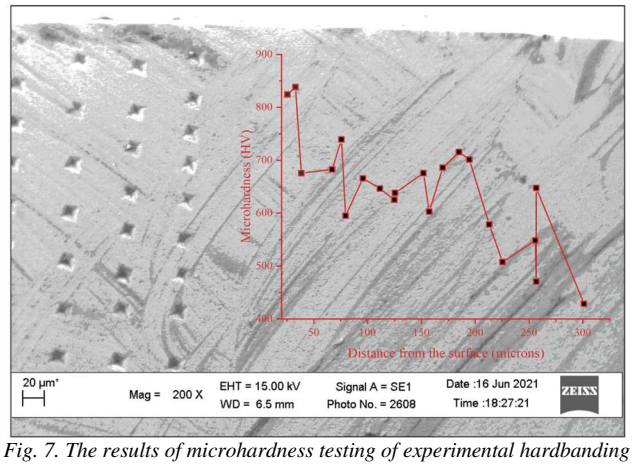

Fig. 7. The results of microhardness testing of experimental hardbanding

Hardbanding of the joints of drill pipes, which were subjected to industrial tests, was performed using a hardbanding machine (Fig. 8, a), the units for automatic feeding of the flux-cored wire to the welding zone, the power supply and the mechanism for supporting and holding the drill pipes includes rotation. For hardbanding (Muravev et al., 2019, Bozek et al., 2016), a drill pipe with worn hardbanding (high-chromium alloy) was used (Kopas et al., 2017). The wear was determined by visual inspection prior to the reapplication of drilling pipes (Saga, Vasko, 2009). Due to the high compatibility of high manganese austenite with a wide range of alloys,

including high chromium, experimental alloy hardbanding was performed over the worn surfaces, allowing them to be re-used with approximately the same durability.

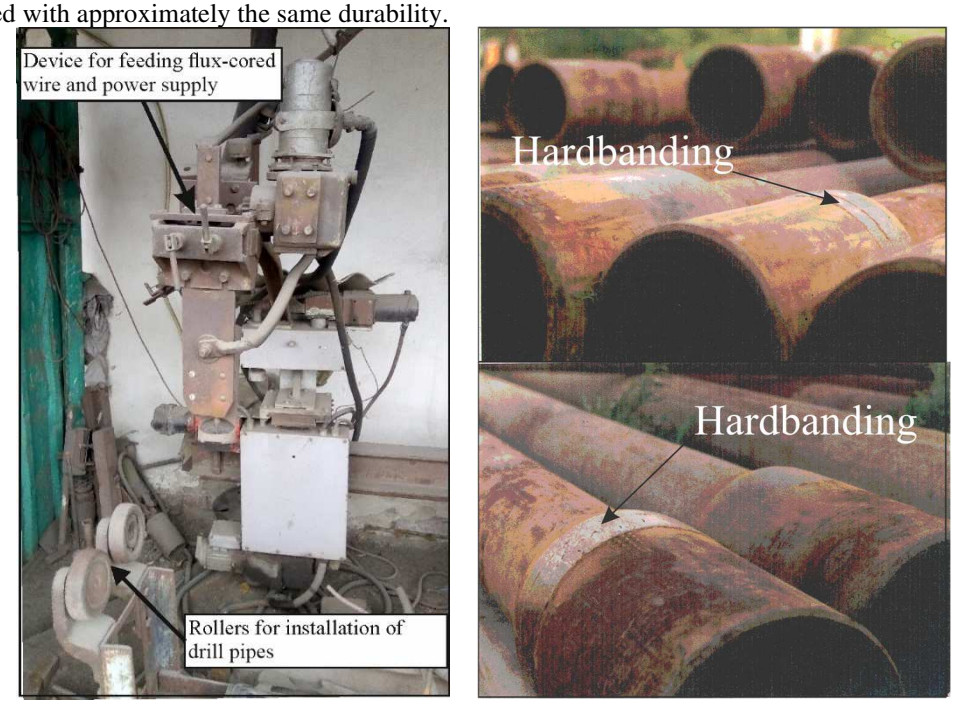

Fig. 8. The general view of the hardbanding machine (a) and the recovered drill pipes (b)

Discussion

Due to its high metallurgical compatibility with certain steels and with the Fe-based alloys having high amounts of the alloying elements, the developed hardbanding alloy based on high-manganese austenite offers the possibility of re-using drill pipes with previously worn deposited layers. Such a combination of properties is achieved by using the complex alloy system, which makes it possible to solve the following tasks: prevention of the formation of a continuous cementite network at the austenite grain boundaries by replacing it with discontinuous layers of (Mo,V) C and creating the conditions for structure formation with matrix reinforcements. Complex (Nb,Ti,Mo,V) C carbides used as reinforcements have increased values of microhardness and crack resistance with respect to the corresponding monocarbides and precipitates in the form of fine grains preventing the intensive wear of the counter body (casing) during the friction. Complex (Nb,Ti,Mo,V) C carbides used as reinforcements have higher values of microhardness and crack resistance compared to the corresponding monocarbides and precipitate in the form of fine grains, which prevent intensive wear of the counter body (casing) during the drilling process, unlike WC-based hardbanding materials which cause extreme wear on the casing making their use very limited. In addition, the total amount of the complex carbides in the structure is ~ 30% by volume, which provides a sufficient level of abrasion wear resistance.

One of the most important properties of the proposed hardbanding alloy is the ability for work hardening, which occurs in friction conditions in proportion to the applied load, increasing wear resistance in the most stressed areas without cracking in the deposited layer, as well as at interfaces between the base metal and hardbanding.

The process of hardbanding by FCAW using the proposed alloy is simple, does not require highly skilled personnel and can be easily automated using standard equipment such as standard welding rectifiers that produce a welding current in the range of 160-250 A.

Conclusions

Based on the thermodynamic modelling within the CALPHAD approach as implemented in the Thermo-Calc software used for the multi-component Fe-Mn-Nb-Ti-Mo-V-C system, the composition of the hardbanding alloy of high-manganese steel – refractory compound system proposed. In order to obtain the thermodynamic parameters determining the solid-state solubility of Mn in refractory carbides of MC-type, the first – principles calculations for the special quasi-random model structures were performed using the ATAT software. The experimental results of the microstructural observations of the experimental alloy and the phase composition predicted by thermodynamic modelling agree well, which allows for expanding the composition and temperature ranges for alloy development.

FCAW hardbanding with cored wire containing ferromanganese and powders of NbC, TiC, Mo_2C and VC in equimolar proportions was tested against the commercially available Fe-W-C and Fe-Cr-C based hardfacing alloys and showed the best values of the properties preventing casing wear together with sufficient abrasion resistance. Despite the highest wear resistance of Fe-W-C alloys in both cases (abrasion and against the steel counter body), they cause extremely high wear to the casing, which makes them unsuitable for wide use.

Based on the results, further research in materials development makes sense in the direction of developing materials based on manganese steel and multi-component carbides additionally alloyed with chromium and nickel to ensure the durability of coatings when working in aggressive environments.

References

Abd Ali, L.M., Ali, Q.A., Klačková, I., Issa, H.A., Yakimovich, B.A., Kuvshimov, V. (2021). Developing a thermal design for steam power plants by using concentrating solar power technologies for a clean environment. Acta Montanistica Slovaca, vol. 26 (4), 2021, pp. 773-783, 2021, DOI https://doi.org/10.46544/AMS.v26i4.14, 2021

Abramov, I., Bozek, P., Nikitin, Y., Abramov, A., Sosnovich, E., Stollmann. (2015). Diagnostics of electrical drives. In The 18th International Conference on Electrical Drives and Power Electronics . EDPE 2015. The High Tatras, Slovakia, 21 - 23. September 2015, pp. 364-367. DOI: 10.1109/EDPE.2015.7325321

Andersson, J.-O., Helander, T., Höglund, L., Shi, P., & Sundman, B. (2002). Thermo-Calc & DICTRA, computational tools for materials science. Calphad, 26(2), 273–312. https://doi.org/10.1016/s0364-5916(02)00037-8

Bazaluk, O., Dubei, O., Ropyak, L., Shovkoplias, M., Pryhorovska, T., & Lozynskyi, V. (2022). Strategy of compatible use of jet and plunger pump with chrome parts in oil well. Energies, 15(1). https://doi.org/10.3390/en15010083

Bazaluk, O., Slabyi, O., Vekeryk, V., Velychkovych, A., Ropyak, L., & Lozynskyi, V. (2021). A technology of hydrocarbon fluid production intensification by productive stratum drainage zone reaming. Energies, 14(12). https://doi.org/10.3390/en14123514

Bazaluk, O., Velychkovych, A., Ropyak, L., Pashechko, M., Pryhorovska, T., & Lozynskyi, V. (2021). Influence of heavy weight drill pipe material and drill bit manufacturing errors on stress state of steel blades. Energies, 14(14). https://doi.org/10.3390/en14144198

Bembenek, M., Krawczyk, J., & Pańcikiewicz, K. (2020). The wear on roller press rollers made of 20Cr4/1.7027 steel under conditions of copper concentrate briquetting. Materials, 13(24), 5782.

Bozek, P., Lozkin, A., Gorbushin, A. (2016). Geometrical method for increasing precision of machine building parts. In Procedia Engineering, International Conference on Manufacturing Engineering and Materials, ICMEM 2016, 6. - 10. June 2016, Nový Smokovec, Slovakia. Vol. 149. DOI: doi: 10.1016/j.proeng.2016.06.708

Burduk, A., Wiecek, D., Tlach, V., Ságová, Z., Kochanska, J. (2021). Risk assessment of horizontal transport system in a copper mine. Acta Montanistica Slovaca, vol. 26 (2), 2021, DOI 10.46544/AMS.v26i2.09, 2021

Caltaru, M. M., Ripeanu, R. G., Badicioiu, M., & Zisopol, D. G. (2020). Experimental researches to establish the optimum hardbanding technology and materials of the heavy weight drill pipe. MATEC Web of Conferences, 318, 01017.

Cernecky, J., Bozek, P., Pivarciova, E. (2015) A new system for measuring the deflection of the beam with the support of digital holographic interferometry. In Journal of Electrical Engineering. Vol. 66, Iss. 1 (2015), pp. 53-56

Dychkovskyi, R., Shavarskyi, I., Saik, P., Lozynskyi, V., Falshtynskyi, V., & Cabana, E. (2020). Research into stress-strain state of the rock mass condition in the process of the operation of double-unit longwalls. Mining of Mineral Deposits, 14(2), 85–94. https://doi.org/10.33271/mining14.02.085

Garrity, K. F., Bennett, J. W., Rabe, K. M., & Vanderbilt, D. (2014). Pseudopotentials for high-throughput DFT calculations. Computational Materials Science, 81, 446–452. https://doi.org/10.1016/j.commatsci.2013.08.053

Giannozzi, P., Baroni, S., Bonini, N., Calandra, M., Car, R., Cavazzoni, C., Ceresoli, D., Chiarotti, G. L., Cococcioni, M., Dabo, I., & others. (2009). QUANTUM ESPRESSO: a modular and open-source software project for quantum simulations of materials. Journal of Physics: Condensed Matter, 21(39), 395502.

Haberer, J. F., Gates, J., & Fifield, R. (2014). Resistance to Abrasive Wear and Metallurgical Property Assessment of Nine Casing-Friendly Hard-Banding Alloy Chemistries: Abrasion Resistance Assessment Using ASTM G65 Methodology (Standard Test Method for Measuring Abrasion with Dry Sand/Rubber Wheel Apparatus). All Days. https://doi.org/10.2118/170520-ms

Hallstedt, B., Khvan, A. V., Lindahl, B. B., Selleby, M., & Liu, S. (2017). PrecHiMn-4—A thermodynamic database for high-Mn steels. Calphad, 56, 49–57. https://doi.org/10.1016/j.calphad.2016.11.006

Handrik, M., Kopas, P., Baniari, V., Vasko, M., Saga, M. (2017). Analysis of stress and strain of fatigue specimens localised in the cross-sectional area of the gauge section testing on bi-axial fatigue machine loaded in the high-cycle fatigue region. XXI Polish-Slovak Scientific Conference Machine Modeling and Simulations MMS 2016, Hucisko, Poland, 6-8 sept. 2016, Procedia Engineering, vol. 177, pp. 516-519, DOI 10.1016/j.proeng.2017.02.254, 2017

Hillert, M. (2001). The compound energy formalism. Journal of Alloys and Compounds, 320(2), 161–176. https://doi.org/10.1016/s0925-8388(00)01481-x

Khouri, S., Pavolová, H., Cehlár, M., & Bakalár, T. (2016). Metallurgical brownfields re-use in the conditions of Slovakia—A case study. Metalurgija, 55(3), 500–502.

Klarák, J., Andok, R., Hricko, J., Klačková, I., Tsai, H.-Y. (2022). Design of the Automated Calibration Process for an Experimental Laser Inspection Stand. Sensors 2022, 22, 5306, https://doi.org/10.3390/s22145306, 2022

Kopas, P., Blatnicky M., Saga M., Vasko, M. (2017). Identification of mechanical properties of weld joints of AlMgSi07.F25 Aluminium Alloy. Metalurgija, vol. 56 (1-2), 2017, pp. 99-102, 2017

Kopas, P., Saga, M., Baniari, V., Vasko, M., Handrik, M. (2017). A plastic strain and stress analysis of bending and torsion fatigue specimens in the low-cycle fatigue region using the finite element methods. XXI Polish-Slovak Scientific Conference Machine Modeling and Simulations MMS 2016, Hucisko, Poland, 6-8 sept. 2016, Procedia Engineering, vol. 177, pp. 526-531, DOI 10.1016/j.proeng.2017.02.256, 2017

Kovanič, Ľ., Blistan, P., Rozložník, M. and Szabó, G. UAS RTK / PPK photogrammetry as a tool for mapping the urbanized landscape, creating thematic maps, situation plans and DEM. Acta Montanistica Slovaca. 2021, Volume 26 (4) 649-660 DOI: https://doi.org/10.46544/AMS.v26i4.05

Kovanič, Ľ.; Blistan, P.; Štroner, M.; Urban, R.; Blistanova, M. Suitability of Aerial Photogrammetry for Dump Documentation and Volume Determination in Large Areas. *Appl. Sci.* **2021**, *11*, 6564. https://doi.org/10.3390/app11146564

Kopei, V., Onysko, O., & Panchuk, V. (2019). Computerized system based on FreeCAD for geometric simulation of the oil and gas equipment thread turning. IOP Conference Series: Materials Science and Engineering, 477(1), 012032.

Kopei, V., Onysko, O., & Panchuk, V. (2020). Principles of development of product lifecycle management system for threaded connections based on the Python programming language. Journal of Physics: Conference Series, 1426(1), 012033.

Kopei, V., Onysko, O., Panchuk, V., Pituley, L., & Schuliar, I. (2021). Influence of Working Height of a Thread Profile on Quality Indicators of the Drill-String Tool-Joint. Grabchenko's International Conference on Advanced Manufacturing Processes, 395–404.

Kuric, I., Klačková, I., Domnina, K., Stenchlák, V., Sága, M. jr. (2022). Implementation of Predictive Models in Industrial Machines with Proposed Automatic Adaptation Algorithm. Applied Sciences - Basel, Mdpi, 2022, vol. 12 (4), 1853, ISSN 2076-3417, DOI.org/10.3390/app12041853, 2022

Kuric, I., Klačková, I., Nikitin, Y.R., Zajačko, I., Císar, M., Tucki, K. (2021). Analysis of diagnostic methods and energy of production systems drives, Processes, Mdpi, 9, 843, DOI.org/10.3390/pr9050843, 2021

Kuric, I., Tlach, V., Císar, M., Ságová, Z., Zajačko, I. (2020). Examination of industrial robot performance parameters utilizing machine tool diagnostic methods. In International Journal of Advanced Robotic Systems, 17 (1), 2020, DOI 10.1177/1729881420905723, 2020

Kusyi, Y., & Kuk, A. (2020). Investigation of the technological damageability of castings at the stage of design and technological preparation of the machine Life Cycle. Journal of Physics: Conference Series, 1426(1), 012034.

Levchuk, K. G. (2017). Investigation of the vibration transfer process to a stuck drill string. SOCAR Proceedings, 2, 23–33. https://doi.org/10.5510/ogp20170200312

Levchuk, K. H., Radchenko, and T. M., Tatarenko, V. A., & and. (2021). High-Temperature Entropy Effects in Tetragonality of the Ordering Interstitial–Substitutional Solution Based on Body-Centred Tetragonal Metal. Metallofizika I Noveishie Tekhnologii, 43(1), 1–26. https://doi.org/10.15407/mfint.43.01.0001

Mandryk, O., Vytyaz, O., Poberezhny, L., & Mykhailiuk, Y. (2020). Increase of the technogenic and ecological safety of the natural gas transportation due to displacement of explosive mixtures with nitrogen. Archives of Materials Science and Engineering, 106(1).

Medvid, I., Onysko, O., Panchuk, V., Pituley, L., & Schuliar, I. (2020). Kinematics of the Tapered Thread Machining by Lathe: Analytical Study. Grabchenko's International Conference on Advanced Manufacturing Processes, 555–565.

Melnick, O., Soolshenko, V., & Levchuk, K. (2020). Thermodynamic prediction of phase composition of transition metals high-entropy alloys. Metallofizika i Noveishie Tekhnologii, 42(10), 1387–1400.

Moisyshyn, V., & Levchuk, K. (2016). The impact of vibration mechanism'installation place on the process of retrieving stuck drill pipe. Mining of Mineral Deposits, 10, Iss. 3, 65–76.

Moisyshyn, V., Yacyshyn, V., & Vytyaz, O. (2012). The use of the spatial characteristics technique with the view of estimating the explosion wave impact on the stuck drilling string zone. Archives of Mining Sciences, 57(3).

Muravev, V. V., Muraveva, O. V., Volkova, L. V., Sága, M., Ságová, Z. (2019). Measurement of Residual Stresses of Locomotive Wheel Treads During the Manufacturing Technological Cycle. Management systems in Production Engineering, 27 (4) 2019, DOI 10.1515/mspe-2019-0037, 2019

Murthy, G., Das, G., Das, S. K., Parveen, N., & Singh, S. (2011). Hardbanding failure in a heavy weight drill pipe. Engineering Failure Analysis, 18(5), 1395.

Onysko, O., Kopei, V., Panchuk, V., Medvid, I., & Lukan, T. (2020). Analytical Study of Kinematic Rake Angles of Cutting Edge of Lathe Tool for Tapered Thread Manufacturing. In Lecture Notes in Mechanical Engineering (pp. 236–245). Springer International Publishing. https://doi.org/10.1007/978-3-030-40724-7_24

Pashechko, M., Józwik, J., Dziedzic, K., Karolus, M., & Usydus, I. (2017). Surface Hardening of HS6-5-2 Quick-Cutting Steel in the Course of Chemical Thermal Treatment. Materials Science, 52(6), 834–840. https://doi.org/10.1007/s11003-017-0028-4

Peterka, J., Pokorný, P. & Vaclav, S. (2008). CAM strategies and surfaces accuracy, 19th Int. Symp. of Danube Adria Association for Automation and Manufacturing. Annals of DAAAM and Proceedings. 1061-1062

Pryhorovska, T., & Ropyak, L. (2019). Machining Error Influnce on Stress State of Conical Thread Joint Details. Proceedings of the International Conference on Advanced Optoelectronics and Lasers, CAOL, 2019-September, 493–497. https://doi.org/10.1109/CAOL46282.2019.9019544

Pukanská, K., Bartoš, K., Bella, P., Rákay ml, Š., & Sabová, J. (2017). Comparison of non-contact surveying technologies for modelling underground morphological structures. Acta Montanistica Slovaca, 22(3), 246–256.

Radchenko, T., Gatsenko, O., Lizunov, V., & Tatarenko, V. (2020). Martensitic α ″-Fe 16 N 2-Type Phase of Non-Stoichiometric Composition: Current Status of Research and Microscopic Statistical-Thermodynamic Model, Prog. Phys. Met, 21, 580–618.

Romanyshyn, T., Romanyshyn, L., Bembenek, M., & Mokhnii, I. (2020). Assessment of the Technical Level of Magnetic Fishing Tools. Management Systems in Production Engineering, 28(2), 78–83. https://doi.org/10.2478/mspe-2020-0012

Ropyak, L. Y., Vytvytskyi, V., Velychkovych, A., Pryhorovska, T., & Shovkoplias, M. (2021). Study on grinding mode effect on external conical thread quality. IOP Conference Series: Materials Science and Engineering, 1018(1), 012014.

Ropyak, L. Ya., Makoviichuk, M. V., Shatskyi, I. P., Pritula, I. M., Gryn, L. O., & Belyakovskyi, V. O. (2020). Stressed state of laminated interference-absorption filter under local loading. Functional Materials, 27(3), 638–642. https://doi.org/10.15407/fm27.03.638

Saakiyan, L. S., Efremov, A. P., Ropyak, L. Ya., & Gorbatskii, A. V. (1987). A method of microelectrochemical investigations. Soviet Materials Science, 23(3), 267–269. https://doi.org/10.1007/BF00720884

Shats'kyi, I., Shopa, V., & Velychkovych, A. (2021). Development of full-strength elastic element section with open shell. Strength of Materials, 53(2), 277–282.

Saga M., Blatnicka M., Blatnicky M., Dizo J., Gerlici J. (2020). Research of the Fatigue Life of Welded Joints of High Strength Steel S960 QL Created Using Laser and Electron Beams, Materials, vol.13 (11), Article No. 2539, DOI 10.3390/ma13112539, 2020

Saga M., Blatnicky M., Vasko M., Dizo J., Kopas P., Gerlici J. (2020). Experimental Determination of the Manson-Coffin Curves for an Original Unconventional Vehicle Frame. Materials, vol.13 (20), Article No. 4675, DOI 10.3390/ma13204675, 2020

Saga M., Jakubovicova L. (2014). Simulation of vertical vehicle non-stationary random vibrations considering various speeds, Scientific Journal of Silesian University of Technology-Series Transport. Vol. 84, pp. 113-118, 2014

Saga, M., Vasko, M. (2009). Stress sensitivity analysis of the beam and shell finite elements. Komunikacie, vol. 11 (2), pp 5-12, ISSN 1335-4205, 2009

Sapietova, A., Saga, M., Novak, P., Bednar, R., Dizo, J. (2011). Design and Application of Multi-software Platform for Solving of Mechanical Multi-body System Problems. Mechatronics: Recent Technological and Scientific Advances. 9th International Conference on Mechatronics, Warsaw, Poland, sep. 21-24, 2011, pp. 345-354, 2011

Segota, SB., Andelic, N., Lorencin, I., Saga M., Car, Z. (2020). Path planning optimization of six-degree-of-freedom robotic manipulators using evolutionary algorithms. International journal of advanced robotic systems, vol.17 (2), DOI 10.1177/1729881420908076, 2020

Shats'kyi, I. (2015). Limiting equilibrium of a plate with partially healed crack. Materials Science, 51(3), 322–330.

Shihab, T., Prysyazhnyuk, P., Semyanyk, I., Anrusyshyn, R., Ivanov, O., & Troshchuk, L. (2020). Thermodynamic Approach to the Development and Selection of Hardfacing Materials in Energy Industry. Management Systems in Production Engineering, 28(2), 84–89. https://doi.org/10.2478/mspe-2020-0013

Shyrokov, V., Vasyliv, K. B., Duryahina, Z., Laz'Ko, H., & Rats'Ka, N. (2009). Effect of laser microalloying with niobium on the wear resistance of stainless steels. Materials Science, 45(4), 473–480.

Tatarenko, V., & Radchenko, T. (2003). The application of radiation diffuse scattering to the calculation of phase diagrams of FCC substitutional alloys. Intermetallics, 11(11–12), 1319–1326.

Teodoriu, C., & Bello, O. (2021). An Outlook of Drilling Technologies and Innovations: Present Status and Future Trends. Energies, 14(15). https://doi.org/10.3390/en14154499

van de Walle, A., & Asta, M. (2019). High-throughput calculations in the context of alloy design. MRS Bulletin, 44(4), 252–256.

Vytyaz, O., Chudyk, I., & Mykhailiuk, V. (2015). Study of the effects of drilling string eccentricity in the borehole on the quality of its cleaning. In New Developments in Mining Engineering 2015: Theoretical and Practical Solutions of Mineral Resources Mining. CRC Press. https://www.scopus.com/inward/record.uri?eid=2-s2.0-85053652500&partnerID=40&md5=3f481bf2ba53f28d9de18983cb81d24d

Vaclav, S., Peterka, J. & Pokorny, P. (2007). Objective method for assembly. 18th Int. Symp. of Danube Adria Association for Automation and Manufacturing. Annals of DAAAM for 2007 & Proceedings of the 18th Int. DAAAM Symp. Intelligent manufacturing & automation: focus on creativity, responsibility, and ethics of engineers. 797-498

Walle, A., & Ceder, G. (2002). Automating first-principles phase diagram calculations. Journal of Phase Equilibria, 23(4), 348–359. https://doi.org/10.1361/105497102770331596

Walle, A. van de, Nataraj, C., & Liu, Z.-K. (2018). The Thermodynamic Database Database. Calphad, 61, 173–178. https://doi.org/10.1016/j.calphad.2018.04.003

Walle, A. van de, Sun, R., Hong, Q.-J., & Kadkhodaei, S. (2017). Software tools for high-throughput CALPHAD from first-principles data. Calphad, 58, 70. https://doi.org/10.1016/j.calphad.2017.05.005

Wiecek, D., Burduk, A., Kuric, I. (2019). The use of ANN in improving efficiency and ensuring the stability of the copper ore mining process. Acta Montanistica Slovaca, vol. 24 (1), pp. 1–14, 2019.

Zhang, K., Wang, Z., & Wang, D. (2020). Research Progress of the Drill String Hardbanding Materials. In Strength of Materials. IntechOpen. https://doi.org/10.5772/intechopen.90013